Electronic Supplementary Material (ESI) for Chemical Communications.
This journal is © The Royal Society of Chemistry 2018

Supplementary Information

High-temperature growth of thick-shell CdSe/CdS core/shell nanoplatelets

Aurelio A. Rossinelli[a], Andreas Riedinger[ab], Patricia Marqués-Gallego[a], Philippe N. Knüsel[a], Felipe V. Antolinez[a], and David J. Norris*[a]

[a]Optical Materials Engineering Laboratory, Department of Mechanical and Process Engineering, ETH Zurich, 8092 Zurich, Switzerland. E-mail: dnorris@ethz.ch

[b]Max Planck Institute for Polymer Research, Ackermannweg 10, 55128 Mainz, Germany

Materials

1-octadecene (ODE, 90%, #O806), 1-octanethiol (≥ 98.5%, #471836), 2-propanol (≥ 99.9%, #34965), acetonitrile (≥ 99.9%, #34998), cadmium acetate dihydrate [Cd(acetate)$_2$ dihydrate, 98%, #289159], methyl acetate (≥ 98%, #W267600), myristic acid (≥ 98%, #70082), oleic acid (OA, 90%, #364525), oleylamine (OAm, 70%, #O7805), selenium (≥ 99.5%, #209651), trifluoroacetic acid (≥ 99.0%, #302031), and trifluoroacetic anhydride (≥ 99%, #106232) were purchased from Sigma Aldrich. Cadmium oxide (99.999%, #48-0800) was obtained from Strem Chemicals. Triethylamine (99%, #157910010) was acquired from Acros Organics. n-hexane and methanol were purchased from Thommen-Furler AG, and absolute ethanol from Alcosuisse AG. [2-[2-[4-(dimethylamino)phenyl]ethenyl]-6-methyl-4H-pyran-4-ylidene]-propanedinitrile (DCM, #06490) was received from Exciton. All chemicals were used without further purification, except where noted.

Synthetic Methods

Preparation of cadmium myristate [Cd(myristate)$_2$] and cadmium oleate [Cd(oleate)$_2$]. Cadmium carboxylates were synthesized following a modified protocol by Hendricks *et al.*[S1] Briefly, 5.75 g CdO and 20 ml acetonitrile were combined in a 100-ml round-bottom flask and the mixture was stirred and cooled in an ice bath. Then, 0.7 ml trifluoroacetic acid and 6.2 ml of trifluoroacetic anhydride were added. After 10 min, the ice bath was removed and the flask heated at 50 °C until the solution turned white. In a 500-ml Erlenmeyer flask, 20.6 g myristic acid (or 28.6 ml oleic acid), 180 ml 2-propanol, and 14.0 ml of triethylamine were mixed and stirred. The cadmium trifluoroacetate solution was then slowly added to the myristic acid (or oleic acid) solution while stirring. The resulting white precipitate was vacuum-filtered through a fritted glass funnel and rinsed thoroughly with methanol. The final product was dried in a vacuum oven at 40 °C and stored under ambient conditions.

Synthesis of 4-monolayer-thick (4 ML) CdSe nanoplatelets (NPLs). Our CdSe NPL synthesis was slightly modified from a protocol by Tessier *et al.*[S2] Briefly, 170 mg Cd(myristate)$_2$, 12 mg Se powder (stored in a N_2-filled glove box), and 15 ml ODE were added to a 100-ml round-bottom flask and degassed under vacuum for 30 min. Then, the mixture was heated up to 240 °C under N_2. At 200 °C, 80 mg Cd(acetate)$_2$ dihydrate was added. The mixture was kept at 240 °C for 8 min. Afterwards, the reaction flask was cooled using an air gun to 160 °C. During this cooling step, 0.5 ml OA was added when the temperature reached 185 °C. Once at 160 °C, the flask was placed in a water bath and cooled to room temperature (RT), and then 5 ml hexane was added. The mixture was centrifuged at 8000 rpm (8586 g) for 10 min. The precipitate was re-dispersed in 5 ml hexane and centrifuged at 7000 rpm (6574 g) for 7 min. Unwanted 3-monolayer-thick NPLs were removed as the precipitate. The 4-monolayer-thick NPLs in the supernatant were then stored in the dark under ambient conditions until needed. This synthesis typically produced 4-ML NPLs with lateral sizes of approximately 20 x 20 nm. For the shell synthesis, the NPLs were precipitated from the hexane dispersion by adding methyl acetate and centrifuging at 7000 rpm (6574 g) for 7 min.

Synthesis of CdSe/CdS core/shell nanoplatelets (NPLs). In a typical synthesis, 4 ML CdSe NPLs [an amount equivalent to 1 ml of NPL dispersion with an optical density (OD) of 20 at the lowest energy excitonic peak, assuming a 1-cm optical path length], 5 ml ODE, and 135 mg Cd(oleate)$_2$ (0.2 mmol) were added to a 100-ml round-bottom flask. The mixture was degassed under vacuum for 40 min at RT and 20 min at 80 °C. Afterwards, 1 ml OAm (stored in a N_2-filled glovebox) was added and the temperature was raised to 300 °C under N_2 at a rate of ~15 °C/min. Starting at 180 °C, a solution of 42 µl 1-octanethiol (0.24 mmol) dissolved in 6 ml ODE was injected at a rate of 3 ml/h. After the injection, the solution was cooled down, and 5 ml hexane was added. The core/shell NPLs were separated from the CdS and CdO side products by selective precipitation. (See below for a discussion of CdO formation.) In a first step, the mixture was centrifuged at 6000 rpm (4830 g) for 10 min. The core/shell NPLs in the precipitate were re-dispersed in 5 ml hexane with the addition of a small amount (~1 to 2 drops) of OAm. [Core/shell NPLs that remained in the supernatant after this centrifugation step could be precipitated by adding methyl acetate and centrifuging at 6000 rpm (4830 g).] The hexane dispersion of NPLs was centrifuged at 6000 rpm (4830 g) for 7 min to separate the stable core/shell NPLs in the supernatant from CdO and aggregated core/shell NPLs. Then, methyl acetate was added to the supernatant until the mixture turned turbid and it was centrifuged at 6000 rpm (4830 g) for 7 min to remove the smaller-sized CdS side product in the supernatant. A second cycle of the above process (*i.e.* dispersion of the NPLs in hexane followed by precipitation with methyl acetate) was typically used to further purify the product. The core/shell NPLs, re-dispersed in hexane, were then stored in the dark under ambient conditions until needed.

We repeated the above synthesis at injection rates between 1.5 and 3 ml/h. No significant difference in the resulting optical properties could be observed, but controlling etching of the NPL cores was more difficult at slower injection rates. The addition of larger amounts of OAm led to a broader emission peak.

As mentioned above, CdO also forms as a side product. The observed formation of CdO can be explained with the decomposition of Cd-carboxylates at the high temperatures present during the shell growth.[S3] An XRD measurement of the formed side products shows the presence of CdS and CdO (Fig. S10).

Shell growth at higher concentrations. The shell can also be grown using a higher concentration of CdSe NPLs. We increased the concentration up to a factor of 3 [an amount equivalent to 1 ml of NPL dispersion with an optical density (OD) of 60 at the lowest energy excitonic peak, assuming a 1-cm optical path length]. We observed no significant changes in the optical properties of the resulting core/shell NPLs. The high-concentration synthesis only led to a slight reduction in the emission red-shift of a few nanometers (emission peak centered at around 660 nm). To improve the colloidal stability of the particles at these higher concentrations, we slightly modified the protocol by adding 200 µl OA to the reaction mixture of 4 ML CdSe NPLs, 5 ml ODE, and 135 mg Cd(oleate)$_2$ (0.2 mmol) before degassing at room temperature.

Etching experiments. Three etching experiments were performed to evaluate the influence of the reaction conditions on the stability of the CdSe NPLs. Therefore, CdSe NPLs (an amount equivalent to 1 ml of NPL dispersion with an OD of 4.5 at the lowest energy excitonic peak, assuming a 1-cm optical path length) were mixed together with either: (i) 5 ml ODE and 5 ml

OAm, (ii) 10 ml ODE, or (iii) 10 ml ODE and 30.4 mg Cd(oleate)$_2$ (0.045 mmol) in a 100-ml round-bottom flask. The mixture was then degassed under vacuum for 1 h at RT and 20 min at 80 °C. Then, the temperature was raised to 300 °C at a rate of ~15 °C/min and aliquots were taken every 30 °C. The first data points in Fig. 1 in the main text, denoted as "RT", were taken after degassing at room temperature. To enable quantitative comparisons, all optical absorption measurements were performed by diluting 300 µl of the sample in 1800 µl hexane and measured in a 1-cm path-length quartz cuvette.

Characterization Methods

Absorbance. Optical absorption spectra for ultraviolet to visible wavelengths (UV-Vis) were collected using a Varian Cary 50 spectrometer. The measurements were performed by diluting the samples in hexane and using 1-cm path-length quartz cuvettes.

Photoluminescence (PL), photoluminescence excitation (PLE), photoluminescence decays, and photoluminescence quantum yield (QY). PL and PLE spectra were recorded at room temperature using an Edinburgh Instruments FLS 980 fluorometer. For PL spectra presented throughout this work, the excitation wavelength was set to 400 nm. For the PLE data in Fig. S5, the emission was monitored at 680 nm while the excitation wavelength was scanned. For photoluminescence decays, the photoluminescence-lifetime capability of the same fluorometer was used. A pulsed laser diode at 373 nm with a repetition rate of 200 kHz was used as the excitation source. The detected wavelength was set to 515 nm for the core NPLs and 663 nm for the core/shell NPLs. The latter sample had an emission maximum at 663 nm with a fwhm of 22 nm. The detector was the same cooled R928P photomultiplier tube used to collect the PL and PLE results.

QYs were measured with the same fluorometer relative to the standard reference dye DCM using the following equation:[S4]

$$\Phi_x = \Phi_{ref} \cdot \frac{f_{ref}}{f_x} \frac{F_x}{F_{ref}} \frac{n_x^2}{n_{ref}^2},$$

with

$$f = 1 - 10^{-A}$$

where F is the integrated emission signal, n is the refractive index, and A is the absorbance. The subscripts x and ref refer to the NPL dispersion and dye solution, respectively.

For each measurement, three different concentrations were measured with an excitation wavelength of 400 nm (470 nm excitation for DCM) to ensure reliable results. Exciting the core/shell NPLs at 550 nm, which is below the band gap of CdS, led to comparable values for the QY (typically giving an increase of a few percent). The measurements were performed by diluting the samples in hexane and using quartz cuvettes with 1-cm path length.

Transmission electron microscopy (TEM), scanning transmission electron microscopy (STEM), and energy dispersive X-ray spectroscopy (EDS). TEM, STEM, and EDS were performed using an FEI Talos F200X microscope operating at 200 kV. The samples were prepared by drop-casting nanoparticles dispersed in hexane on carbon-coated copper grids.

Powder X-ray diffraction (XRD). XRD measurements were performed using a Bruker D2 Phaser instrument (30 kV, 10 mA, $\lambda_{\mathrm{CuK\alpha}}$ = 1.54184 Å). The samples were drop casted from highly concentrated hexane dispersions onto zero-background Si holders.

Single-nanoplatelet spectroscopy. Samples of CdSe and CdSe/CdS NPLs were treated similarly to allow a fair comparison. Both were precipitated twice with methyl acetate (as described in the Methods section above) to avoid stacking of the platelets. Measurements were then performed by diluting the CdSe and CdSe/CdS NPL stock solutions in hexane by a factor of 10000 and spin coating them onto a microscope cover glass.

To detect single nanoplatelets, an inverted microscope (Nikon, TE200) with a 100x 1.4 numerical aperture oil-immersion objective (CFI Plan Apo VC 100X Oil, 1.4 NA) was used. A white light-emitting diode (Lumencor, Sola SE II light engine) served to illuminate the sample with a dichroic beam splitter (488 nm long pass, AHF Analysentechnik). The NPL emission was collected by the same objective and directed through a 500 nm long-pass emission filter (AHF Analysentechnik) into an imaging spectrometer (Andor, Shamrock 303i). Spectra were obtained by dispersing the emission with a 300 lines/mm grating (500 nm blaze) and detecting the output with an air-cooled electron-multiplying CCD camera (Andor, iXon 888 Ultra). Spatial images for the blinking analysis were obtained with the zero-order diffraction mode of the grating.

For the blinking analysis, images were recorded for 100 s at a frame rate of 20 Hz, yielding 2000 frames. For both core and core/shell NPLs, ten such series were recorded and analyzed identically with a script written in the Python programming language. Each frame was binned by a factor of 4 both horizontally and vertically. Positions of single particles were identified automatically and the emission time traces analyzed. A NPL was considered to be in the ON state in a frame if the number of photon counts detected was larger than 20% of the maximum in the trace. All traces were analyzed in this way to calculate the relative time spent in the ON state.

Supplementary Figures

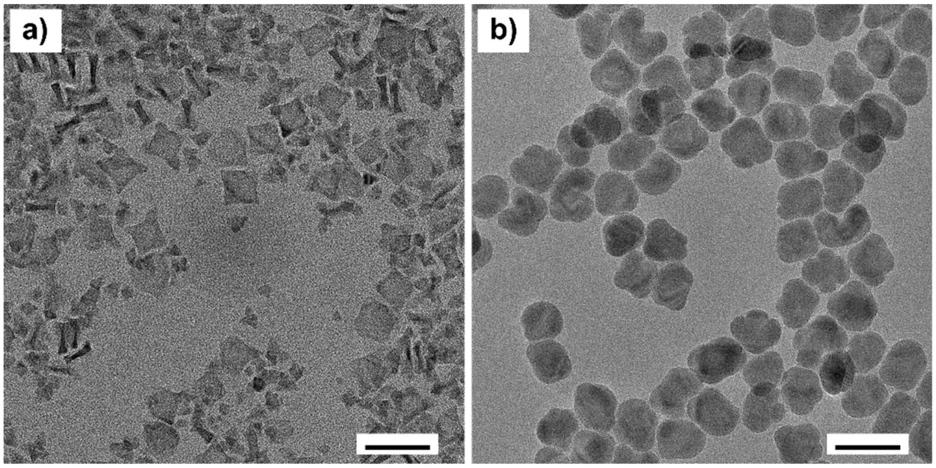

Fig. S1 CdSe/CdS core/shell NPLs with shell growth performed at (a) 265 °C and (b) 315 °C. The lower synthesis temperature leads to anisotropic shells with pronounced growth at the edges of the NPLs while the higher temperature leads to gradual transformation into spherical particles. Black scale bars are 50 nm.

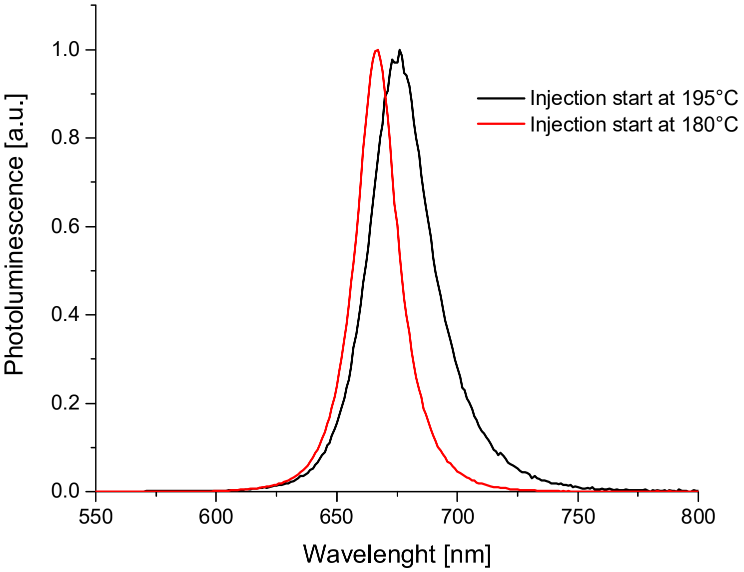

Fig. S2 Influence of the starting temperature of the injection of 1-octanethiol on the emission linewidth. A higher starting temperature results in emission peak broadening.

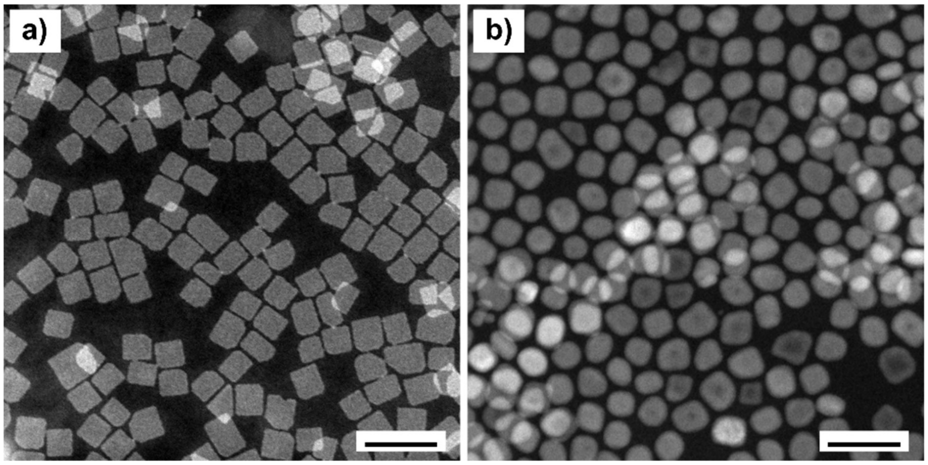

Fig. S3 STEM images of (a) CdSe core NPLs and (b) CdSe/CdS core/shell NPLs. A slight decrease in lateral size can be observed due to slight etching of the NPL cores during the initial stage of the coating. Black scale bars are 50 nm.

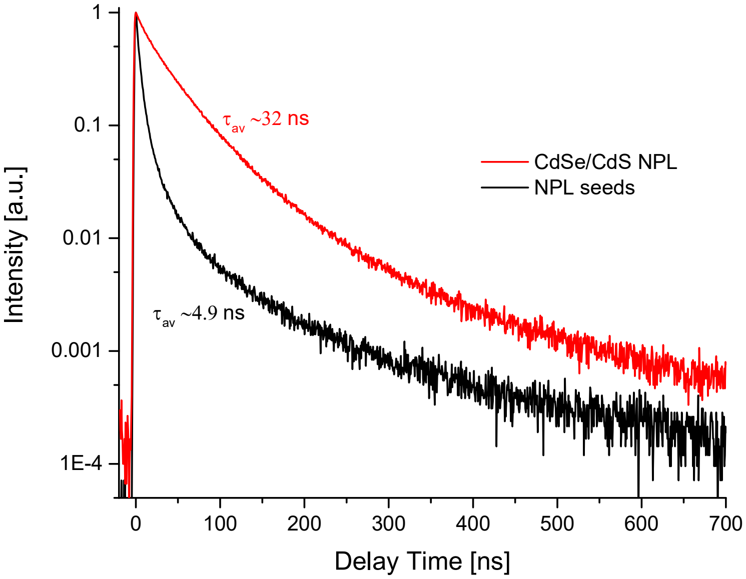

Fig. S4 Room-temperature photoluminescence (PL) decays of CdSe core (black) and CdSe/CdS core/shell (red) NPLs dispersed in hexane. The detected wavelength was set to 515 nm for the core NPLs and 663 nm for the core/shell NPLs. The latter sample had an emission maximum at 663 nm with a fwhm of 22 nm. Due to the delocalization of the electron wave function into the CdS shell, the radiative lifetime in the core/shell NPLs is expected to be longer than in the core NPLs.

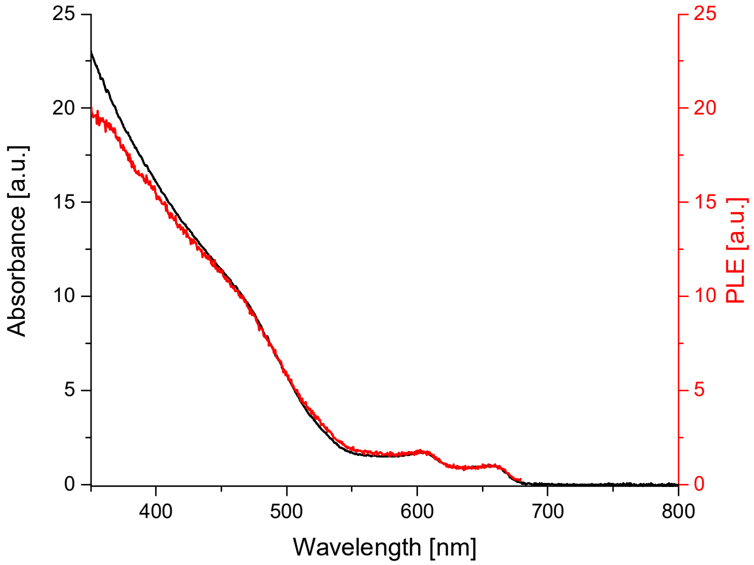

Fig. S5 Optical absorbance (black) and photoluminescence excitation (PLE, red) spectra for CdSe/CdS core/shell nanoplatelets. For PLE, the emission was monitored at 680 nm.

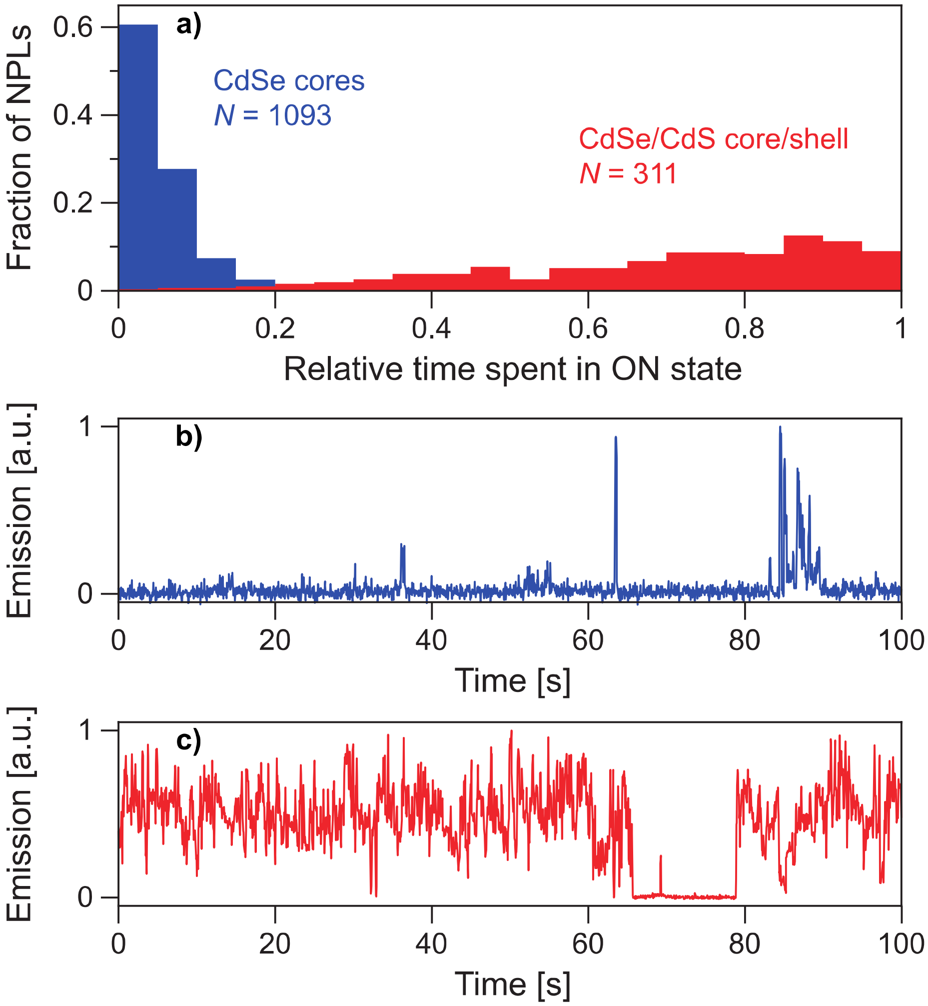

Fig. S6 Single-nanoplatelet room-temperature blinking statistics of CdSe core (blue) and CdSe/CdS core/shell NPLs (red). Clear suppression of fluorescence blinking is observed after the shell growth. (a) Histogram of the NPL blinking behavior at a frame rate of 20 Hz. A particle is defined to be in the ON state if the detected photon count was larger than 20% of its maximum emission intensity. (b,c) Representative emission traces for CdSe core and CdSe/CdS core/shell NPLs, respectively. Statistics were collected on 1093 CdSe and 311 CdSe/CdS NPLs.

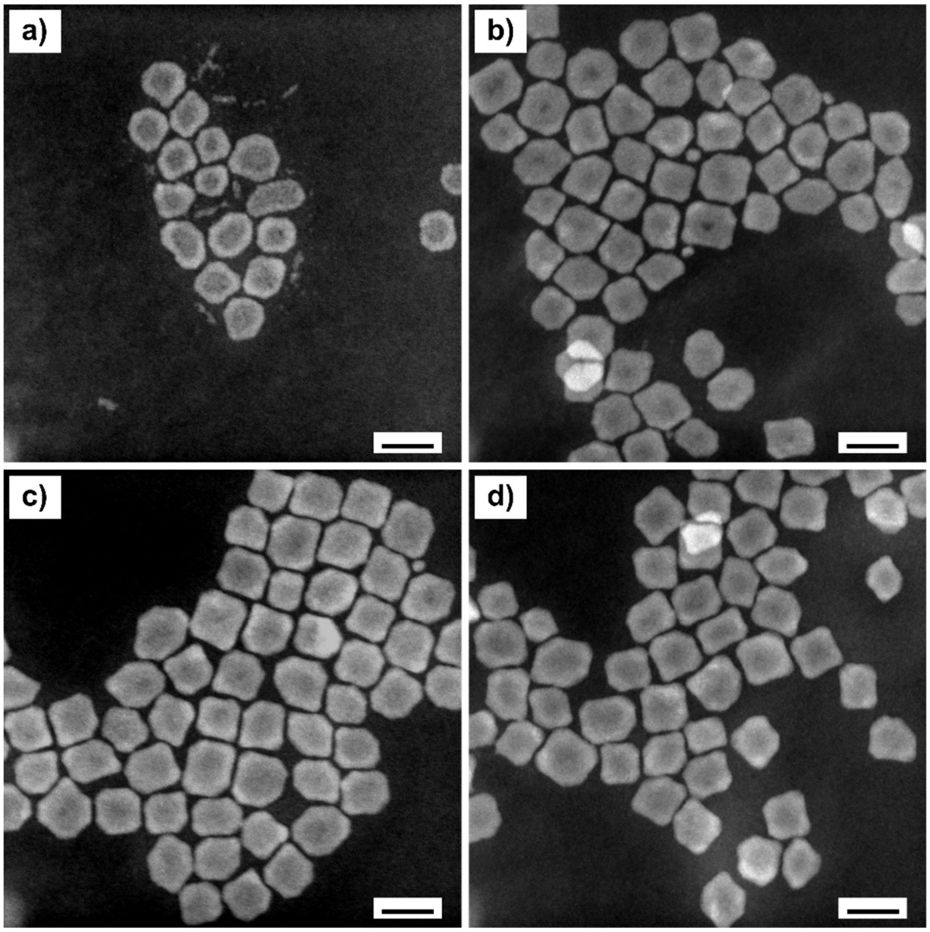

Fig. S7 STEM images of NPLs at different time points during a CdSe/CdS core/shell NPL synthesis with an injection rate of 1-octanethiol of 1.5 ml/h (see Methods above). Aliquots were taken after (a) 15 min, (b) 45 min, (c) 75 min, and (d) 105 min and correspond to the absorption and emission curves shown in Fig. 2a of the main text. The brighter regions on the outer edges of the nanoplatelets observed at early times indicate a slightly increased thickness of the CdS shell. Black scale bars are 25 nm.

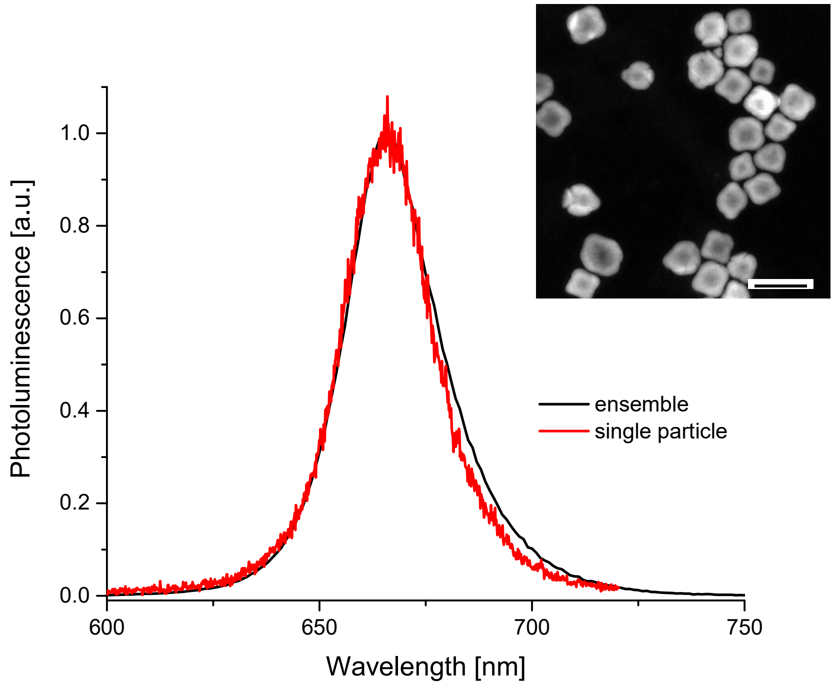

Fig. S8 Comparison of an ensemble and a representative single-nanoplatelet emission linewidth for CdSe/CdS core/shell NPLs with a slight non-uniform shell thickness (inset: STEM image of the corresponding nanoparticles). Both, ensemble and single particles have similar linewidths [ensemble: 26 nm (72 meV); single particles: 25 nm ± 2.2 nm (70 meV ± 6 meV, average of 14 particles)]. The black scale bar is 50 nm.

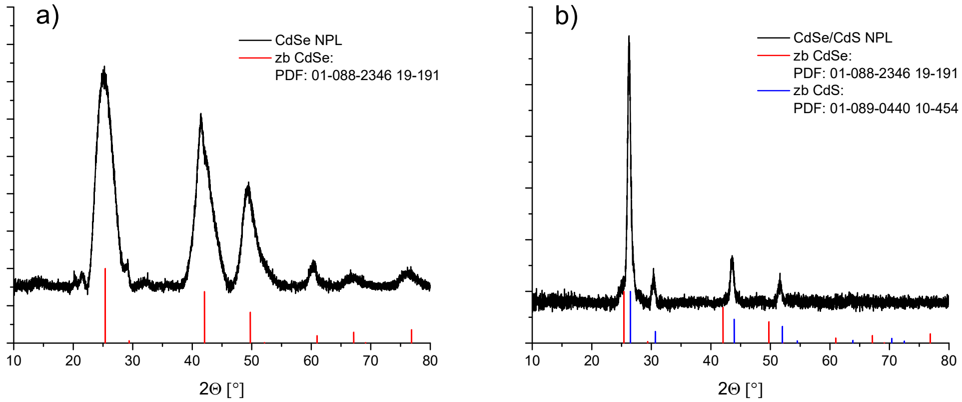

Fig. S9 XRD pattern for (a) CdSe core nanoplatelets and (b) CdSe/CdS core/shell nanoplatelets. Both, core and core/shell NPLs show the cubic (zincblende, zb) phase.

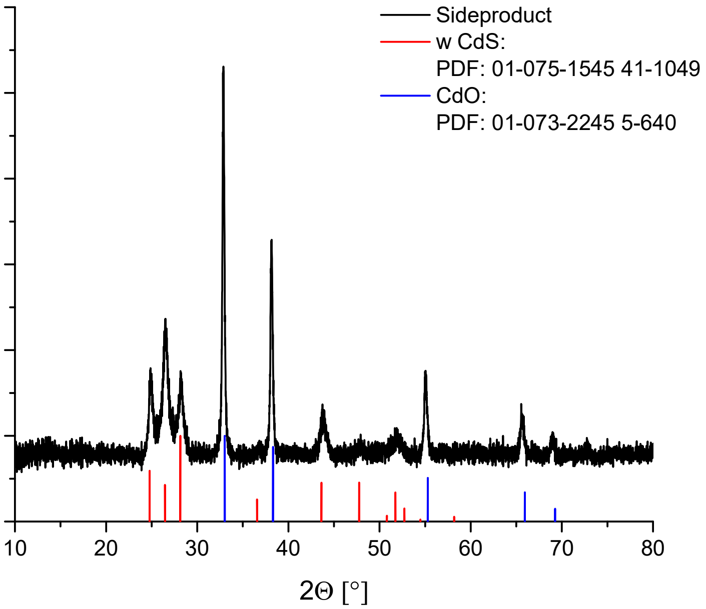

Fig. S10 XRD pattern for the side product formed during the shell synthesis. CdS nanocrystals in the wurtzite phase and CdO were formed. The wurtzite phase of this CdS side product can be distinguished from the cubic phase of the CdS shell in the core/shell NPLs.

Supplementary References

S1 M. P. Hendricks, M. P. Campos, G. T. Cleveland, I. Jen-La Plante and J. S. Owen, *Science*, 2015, **348**, 1226-1230.
S2 M. D. Tessier, L. Biadala, C. Bouet, S. Ithurria, B. Abecassis and B. Dubertret, *ACS Nano*, 2013, **7**, 3332-3340.
S3 R. García-Rodríguez, M. P. Hendricks, B. M. Cossairt, H. Liu and J. S. Owen, *Chem. Mater.*, 2013, **25**, 1233-1249.
S4 K. Rurack and M. Spieles, *Anal. Chem.*, 2011, **83**, 1232-1242.